

pH-Dependent Selective Transfer Hydrogenation of α,β -Unsaturated Carbonyls in Aqueous Media Utilizing Half-Sandwich Ruthenium(II) Complexes

Charles A. Mebi, Radhika P. Nair, and Brian J. Frost*

Department of Chemistry, University of Nevada, Reno, Nevada 89557

Received September 28, 2006

Half-sandwich ruthenium(II) PTA complexes bearing the 1,2-dihydropentalenyl ($C_8H_9^-$, Dp) and indenyl ($C_9H_7^-$, Ind) ancillary ligands have been synthesized and characterized using multinuclear NMR spectroscopy and X-ray crystallography. The complexes $DpRu(PTA)(PPh_3)Cl$, $DpRu(PTA)_2Cl$, $IndRu(PTA)(PPh_3)Cl$, and $[IndRu(PTA)_2(PPh_3)]Cl$ were obtained in good to excellent yields. The solid-state structures of these compounds exhibit piano stool geometries with η^5 -coordination of the indenyl and dihydropentalenyl moieties. $DpRu(PTA)_2Cl$ is water-soluble ($S_{25^\circ C} = 43$ mg/mL), while the mixed phosphine compounds are slightly soluble in acidic solutions. The Ru–H complexes, $Cp'Ru(PTA)(PPh_3)H$ ($Cp' = Ind, Cp$), have been synthesized in good yield and spectroscopically and structurally characterized. The ruthenium hydrides undergo an H/D exchange reaction with CD_3OD with relative rates $CpRu(PTA)(PPh_3)H \gg IndRu(PTA)(PPh_3)H > CpRu(PTA)_2H$. The air-stable $Cp'Ru(PTA)(PR_3)Cl$ complexes ($Cp' = Cp, Dp, Ind$; $PR_3 = PPh_3$ or PTA) exhibit activity in the regioselective transfer hydrogenation of α,β -unsaturated carbonyls in aqueous media with $HCOONa$, $HCOOH$, or isopropanol/ Na_2CO_3 serving as the hydrogen source. They were found to be effective in the selective reduction of the carbonyl functionality of cinnamaldehyde and the C=C bond of benzylidene acetone and chalcone. $IndRu(PTA)(PPh_3)Cl$ was less active than $Cp'Ru(PTA)(PPh_3)Cl$ ($Cp' = Cp$ or Dp). Results of the transfer hydrogenation of unsaturated substrates using $CpRu(PTA)(PPh_3)H$ are also reported.

Introduction

Aqueous biphasic catalysis has been of interest in academic and industrial circles since the early 1970s when Manassen and Joó independently developed the field.^{1,2} Water is probably the most desirable “green” solvent, as it is nonflammable, inexpensive, abundant, and environmentally benign.³ Apart from its role as solvent in aqueous catalysis, water is reported to be actively involved in a variety of reactions through coordination to a metal center and/or proton transfer.⁴ The ability to vary the activity and selectivity of a water-soluble catalyst by modulating conditions, such as pH, is another unique aspect of aqueous phase catalysis.^{4a–7} For example, $Jo\acute{o}^{3a,6–9}$ and others^{10–12}

have reported pH-dependence of the regioselective hydrogenation of α,β -unsaturated carbonyls.

$We^{13,14}$ and others^{15,16} have recently reported that $CpRu(PTA)_2X$ ($X = Cl$ or H) complexes, where PTA = 1,3,5-triaza-7-phosphaadamantane, are active in the catalytic reduction of α,β -unsaturated ketones in aqueous or biphasic environments using H_2 as the reductant. The ability of complexes such as these to undergo H/D exchange with solvent, such as D_2O and CD_3OD , has been reported.^{14,17,18} Herein, we report the preparation and characterization of a series of $Cp'Ru(PTA)(PPh_3)Cl$ complexes bearing 1,2-dihydropentalenyl ($\eta^5-C_8H_9^-$, Dp) or indenyl ($\eta^5-C_9H_7^-$, Ind) ancillary ligands: $DpRu(PTA)(PPh_3)Cl$ (**3**), $IndRu(PTA)(PPh_3)Cl$ (**5**), $[IndRu(PTA)_2(PPh_3)]Cl$ (**6**), and $DpRu(PTA)_2Cl$ (**4**). The use of these compounds as transfer hydrogenation catalysts employing formic acid or sodium

* Corresponding author. E-mail: Frost@chem.unr.edu.

(1) Joó, F.; Beck, M. *Magy. Kém. Foly.* **1973**, *79*, 189–191.

(2) Manassen, J. *Catalysis: Progress in Research*; Plenum Press: London, 1973.

(3) (a) Joó, F. *Acc. Chem. Res.* **2002**, *35*, 738–745. (b) Joó, F. *Aqueous Organometallic Catalysis*; Catalysis by Metal Complexes 23; Kluwer Academic Publishers: Boston, 2001. (c) *Aqueous Organometallic Chemistry and Catalysis*; Horvath, I. T., Joó, F., Eds.; NATO ASI Series 3; High Technology; Kluwer: Dordrecht, The Netherlands, 1995. (d) Joó, F.; Kathó, A. In *Aqueous Phase Organometallic Catalysis*, 2nd ed.; Wiley-VCH: Weinheim, Germany, 2004. (e) Adams, D. J.; Dyson, P. J.; Tavener, S. J. *Chemistry in Alternative Reaction Media*; Wiley: Chichester, U.K., 2004.

(4) For example see: (a) Yin, C.; Xu, Z.; Yang, S.-Y.; Ng, S. M.; Wong, K. Y.; Lin, Z.; Lau, C. P. *Organometallics* **2001**, *20*, 1216–1222. (b) Laghmari, M.; Sinou, D. *J. Mol. Catal.* **1991**, *66*, L15–L18. (c) Kovács, G.; Schubert, G.; Joó, F.; Pápai, I. *Organometallics* **2005**, *24*, 3059–3065. (d) Chu, H. S.; Xu, Z.; Ng, S. M.; Lau, C. P.; Lin, Z. *Eur. J. Inorg. Chem.* **2000**, 993–1000. (e) Ohnishi, Y.; Nakao, Y.; Sato, H.; Sakaki, S. *Organometallics* **2006**, *25*, 3352–3363. (f) Joó, F.; Nadasdi, L.; Benyei, A. Cs.; Darensbourg, D. J. *J. Organomet. Chem.* **1996**, *512*, 45–50.

(5) Joó, F.; Kovacs, J.; Benyei, A. Cs.; Nadasdi, L.; Laurenczy, G. *Chem. Eur. J.* **2001**, *7*, 193–199.

(6) Joó, F.; Kovacs, J.; Benyei, A. Cs.; Katho, A. *Catal. Today* **1998**, *42*, 441–448.

(7) Joó, F.; Kovacs, J.; Benyei, A. Cs.; Katho, A. *Angew. Chem., Int. Ed.* **1998**, *37*, 969–970.

(8) Kovács, G.; Ujaque, G.; Lledós, A.; Joó, F. *Organometallics* **2006**, *25*, 862–872.

(9) Papp, G.; Kovacs, J.; Benyei, A. Cs.; Laurenczy, G.; Nadasdi, L.; Joó, F. *Can. J. Chem.* **2001**, *79*, 635–641.

(10) Joubert, J.; Delbecq, F. *Organometallics* **2006**, *25*, 854–861.

(11) Grosselin, J. M.; Mercier, C.; Allmang, G.; Grass, F. *Organometallics* **1991**, *10*, 2126–2133.

(12) Hernandez, M.; Kalck, P. *J. Mol. Catal. A* **1997**, *116*, 131–146.

(13) Mebi, C. A.; Frost, B. J. *Organometallics* **2005**, *24*, 2339–2346.

(14) Frost, B. J.; Mebi, C. A. *Organometallics* **2004**, *23*, 5317–5323.

(15) Bolano, S.; Gonsalvi, L.; Zanolini, F.; Vizza, F.; Bertolasi, V.; Romero, A.; Peruzzini, M. *J. Mol. Catal. A* **2004**, *224*, 61–70.

(16) Akbayeva, D. N.; Gonsalvi, L.; Oberhauser, W.; Peruzzini, M.; Vizza, F.; Brueggeller, P.; Romero, A.; Sava, G.; Bergamo, A. *Chem. Commun.* **2003**, 264–265.

(17) Belkova, N. V.; Besora, M.; Epstein, L. M.; Lledós, A.; Maseras, F.; Shubina, E. S. *J. Am. Chem. Soc.* **2003**, *125*, 7715–7725.

(18) Kovács, G.; Schubert, G.; Joó, F.; Pápai, I. *Organometallics* **2005**, *24*, 3059–3065.

formate as the reducing agent is described. Also reported is the synthesis and reactivity of the mixed phosphine hydrides CpRu(PTA)(PPh₃)H (**7**) and IndRu(PTA)(PPh₃)H (**8**).

Experimental Section

Materials and Methods. Unless otherwise noted all manipulations were performed on a double-manifold Schlenk vacuum line under nitrogen or in a nitrogen-filled glovebox. Solvents were freshly distilled from standard drying reagents (Na/benzophenone for THF and hexanes; Mg/I₂ for methanol) or dried with activated molecular sieves and degassed with nitrogen, prior to use. Water was distilled and deoxygenated before use. All reagents were obtained from commercial sources, checked by NMR and GC/MS, and used as received. Tetrakis(hydroxymethyl)phosphonium chloride was obtained from Cytec and used without further purification. DpRu(PPh₃)₂Cl,¹⁹ 1,3,5-triaza-7-phosphaadamantane (PTA),^{20,21} CpRu(PPh₃)₂Cl,²² IndRu(PPh₃)₂Cl,²³ and CpRu(PTA)₂Cl^{14,16} were prepared as described in the literature. GC/MS analyses were obtained using a Varian CP 3800 GC (DB5 column) equipped with a Saturn 2200 MS and a CP 8400 auto-injector. All NMR spectra were recorded on either a Varian Unity Plus 500 FT-NMR spectrometer, a Varian NMR System 400, a GN 300 FT-NMR/Scorpio spectrometer, or a QE 300 FT-NMR/Aquarius spectrometer. ¹H and ¹³C NMR spectra were referenced to residual solvent relative to TMS. Phosphorus chemical shifts are relative to an external reference of 85% H₃PO₄ in D₂O with positive values downfield of the reference. IR spectra were recorded on a Perkin-Elmer 2000 FT-IR spectrometer in a 0.1 mm CaF₂ cell for solutions or as a KBr pellet for solid samples. X-ray crystallographic data were collected at 100(±1) K on a Bruker APEX CCD diffractometer with Mo K α radiation (λ = 0.71073 Å) and a detector-to-crystal distance of 4.94 cm. A full sphere of data were collected utilizing four sets of frames, 600 frames per set with 0.3° rotation about ω between frames, and an exposure time of 10 s per frame. Data integration, correction for Lorentz and polarization effects, and final cell refinement were performed using SAINTPLUS and corrected for absorption using SADABS or TWINABS. The structures were solved using direct methods followed by successive least-squares refinement on F^2 using the SHELXTL 5.12 software package.²⁴ Crystallographic data and data collection parameters are listed in Table 1.

Synthesis of (η^5 -C₅H₅)Ru(PTA)(PPh₃)Cl (1**).** CpRu(PTA)(PPh₃)Cl was synthesized by a slightly modified procedure from that recently reported.²⁵ A dichloromethane solution of CpRu(PPh₃)₂Cl (194 mg, 0.27 mmol) and PTA (41 mg, 0.26 mmol) was stirred for 14 h under nitrogen. The reaction mixture was pulled dry under vacuum and washed with diethyl ether, affording 52 mg (0.084 mmol) of **1** as an orange powder in 62% yield. Spectroscopic data for CpRu(PTA)(PPh₃)Cl obtained via this method are identical to those reported in the literature.²⁵

Synthesis of (η^5 -C₈H₉)Ru(PTA)(PPh₃)Cl (3**).** A mixture of DpRu(PPh₃)₂Cl (173 mg, 0.23 mmol) and PTA (36 mg, 0.23 mmol) in 80 mL of toluene was refluxed for 2 h under nitrogen. After cooling to room temperature, the solvent was evaporated and the

solid washed with diethyl ether, affording 76 mg of **3** as orange crystals (50% yield). ¹H NMR (400 MHz, CDCl₃): δ 7.58–7.34 (complex m, PPh₃); 4.41, 4.23 (AB quartet, ²J_{(HAHB)} = 13.2 Hz, 6H NCH₂N); 3.92 (d, ²J_{(HAHB)} = 14.4 Hz 3H, PCH₂N), 3.65 (d, ²J_{(HAHB)} = 14.4 Hz 3H, PCH₂N); 4.24, 3.73, 3.29 (s, 3H Cp); 2.40–1.96 (m, 6H Cp(CH₂)₃). ³¹P{¹H} NMR (162 MHz, CDCl₃): δ 43.2 ppm (d, PPh₃, ²J_{PP}} = 45.2 Hz); –39.6 ppm (d, PTA, ²J_{PP}} = 45.2 Hz). Anal. Calc for C₃₂H₃₆ClN₃P₂Ru: C, 58.14; H, 5.49; N, 6.36. Found: C, 58.41; H, 5.39; N, 6.35. Crystals of **3** obtained from the aforementioned procedure were suitable for X-ray diffraction, details of which may be found in Table 1.}}}

Synthesis of (η^5 -C₈H₉)Ru(PTA)₂Cl (4**).** To 100 mL of toluene was added 173 mg (0.23 mmol) of DpRu(PPh₃)₂Cl along with 78 mg (0.5 mmol) of PTA under nitrogen. The solution was heated to reflux for 3 h, affording DpRu(PTA)₂Cl as a yellow precipitate in 98.5% yield (124 mg, 0.23 mmol). ¹H NMR (300 MHz, CDCl₃): δ 4.59, 4.51 (AB quartet, ²J_{(HAHB)} = 12.8 Hz, 12H NCH₂N); 4.18, 4.17 (m, 3H Cp); 4.16 (d, ²J_{(HAHB)} = 15.6 Hz, 6H PCH₂N); 4.02 (d, ²J_{(HAHB)} = 15.6 Hz, 6H PCH₂N); 2.50–1.96 (m, 6H, Cp(CH₂)₃). ¹H NMR (300 MHz, D₂O): δ 4.52 (br s, 12H NCH₂N); 4.33 (s, 2H, Cp); 4.23 (s, 1H, Cp); 4.09, 3.93 (AB quartet, ²J_{(HAHB)} = 15.9 Hz, 12H PCH₂N); 2.38–1.63 (m, 6H Cp(CH₂)₃). ³¹P NMR (162 MHz, CDCl₃): δ –27.32 ppm (s), ³¹P{¹H} NMR (162 MHz, D₂O): δ –27.15 ppm (s); –26.76 ppm (s). Anal. Calc for C₂₀H₃₃N₆P₂ClRu: C, 43.20; H, 5.98; N, 15.12. Found: C, 43.30; H, 5.75; N, 14.85. Crystals of **4** suitable for X-ray diffraction were obtained by diffusion of diethyl ether into a dichloromethane solution of DpRu(PTA)₂Cl. Crystallographic details are reported in Table 1.}}}}

Synthesis of (η^5 -C₉H₇)Ru(PTA)(PPh₃)Cl (5**).** A mixture of IndRu(PPh₃)₂Cl (1.00 g, 1.3 mmol) and PTA (204 mg, 1.3 mmol) in 105 mL of toluene was refluxed for 5 h under nitrogen. The solvent was removed under vacuum and the residue washed several times with diethyl ether and air-dried, affording **5** as an orange-red solid (312 mg, 72% yield). ¹H NMR (300 MHz, CD₂Cl₂): δ 7.49–7.23 (m, 19H, PPh₃ and indenyl); 7.01 (t, 1H, indenyl); 6.77 (d, 2H, indenyl) 4.35, 4.18 (AB quartet, ²J_{(HAHB)} = 12.9 Hz, PTA, 6H, NCH₂N), 3.91 (d, ²J_{(HAHB)} = 15.0 Hz, PTA, 3H, PCH₂N); 3.54 (d, ²J_{(HAHB)} = 15.0 Hz, PTA, 3H, PCH₂N). ³¹P{¹H} NMR (162 MHz, CD₂Cl₂): δ 50.8 ppm (d, PPh₃, ²J_{PP}} = 42.8 Hz), –22.6 ppm (d, PTA, ²J_{PP}} = 42.8 Hz). Anal. Calc for C₃₃H₃₄N₃P₂ClRu: C, 59.06; H, 5.11; N, 6.26. Found: C, 58.17; H, 5.04; N, 6.35. X-ray-quality crystals of **5** were grown by slow diffusion of diethyl ether into a dichloromethane solution of (η^5 -C₉H₇)Ru(PTA)(PPh₃)Cl. Crystallographic details are presented in Table 1.}}}

Synthesis of [(η^5 -C₉H₇)Ru(PTA)₂(PPh₃)]Cl (6**).** A mixture of IndRuCl(PPh₃)₂ (300 mg, 0.39 mmol) and PTA (122 mg, 0.78 mmol) was refluxed under nitrogen in 40 mL of toluene for 4 h. The resulting yellow precipitate was filtered and dried under vacuum, yielding 197 mg of **6** (62% yield). ¹H NMR (300 MHz, CD₂Cl₂): δ 7.4–7.07 (m, 19H, PPh₃ and indenyl), 7.02 (t, 1H, indenyl); 6.75 (d, 2H, indenyl), 4.40 (s, 12H, PCH₂N); 4.1, 3.8 (AB quartet, ²J_{(HAHB)} = 14 Hz, PTA, 12H, NCH₂N). ³¹P{¹H} NMR (162 MHz, CD₂Cl₂): δ 48.9 ppm (t, PPh₃), –34.1 ppm (d, PTA), ²J_{PP}} = 30.1 Hz. Anal. Calc for C₃₉H₄₆N₆P₃ClRu: C, 56.55; H, 5.60; N, 10.15. Found: C, 56.62; H, 5.60; N, 10.87. [(η^5 -C₉H₇)Ru(PTA)₂(PPh₃)](SnCl₃) was synthesized by stirring a mixture of **6** (58 mg, 0.07 mmol) and SnCl₂·2H₂O (316 mg, 0.14 mmol) in 40 mL of dichloromethane for 14 h under nitrogen. The solution was filtered to remove excess SnCl₂·2H₂O and the solvent evaporated under vacuum, leaving a light brown solid. X-ray-quality crystals of [(η^5 -C₉H₇)Ru(PTA)₂(PPh₃)](SnCl₃) were grown by slow diffusion of diethyl ether into a dichloromethane solution of the ruthenium complex.}

Synthesis of (η^5 -C₅H₅)Ru(PTA)(PPh₃)H (7**).** CpRu(PTA)(PPh₃)Cl (30 mg, 0.05 mmol) and HCO₂Na (7 mg, 0.10 mmol) were refluxed for 1 h under nitrogen in 10 mL of methanol. The

(19) Kirss, R. U.; Ernst, R. D.; Arif, A. M. *J. Organomet. Chem.* **2004**, *689*, 419–428.

(20) Daigle, D. J. *Inorg. Synth.* **1998**, *32*, 40–45.

(21) Daigle, D. J.; Pepperman, A. B. Jr.; Vail, S. L. *J. Heterocycl. Chem.* **1974**, *11*, 407–408.

(22) Joslin, F. L.; Mague, J. T.; Roundhill, D. M. *Organometallics* **1991**, *10*, 521–524.

(23) Oro, L. A.; Ciriano, M. A.; Campo, M.; Foces-Foces, C.; Cano, F. H. *J. Organomet. Chem.* **1985**, *289*, 117–131.

(24) *XRD Single-Crystal Software*; Bruker Analytical X-ray Systems: Madison, WI, 1999.

(25) Romerosa, A.; Campos-Malpartida, T.; Lidrissi, C.; Saoud, M.; Serrano-Ruiz, M.; Peruzzini, M.; Garrido-Cárdenas, J. A.; García-Maroto, F. *Inorg. Chem.* **2006**, *45*, 1289–1298.

Table 1. Crystallographic Data for Complexes 3–8; Cp'Ru(PTA)(PR₃)X, Where Cp' = η^5 -C₅H₅ (Cp), η^5 -C₈H₉, η^5 -C₉H₇ (Ind); X = Cl or H

	(η^5 -C ₈ H ₉)Ru(PTA)(PPh ₃)Cl (3)	(η^5 -C ₈ H ₉)Ru(PTA) ₂ Cl (4)	IndRu(PTA)(PPh ₃)Cl (5)	[IndRu(PPh ₃)(PTA) ₂](SnCl ₃)	CpRu(PTA)(PPh ₃)H (7)	IndRu(PTA)(PPh ₃)H (8)
empirical formula	C ₃₂ H ₃₆ ClN ₃ P ₂ Ru	C ₂₀ H ₃₃ ClN ₆ P ₂ Ru	C ₃₃ H ₃₄ N ₃ P ₂ ClRu	C ₃₉ H ₄₆ N ₆ P ₃ Cl ₃ SnRu	C ₂₉ H ₃₃ N ₃ P ₂ Ru	C ₃₃ H ₃₅ N ₃ P ₂ Ru
fw	661.10	555.98	671.09	1102.76	586.59	636.65
color	orange	yellow	yellow	orange	pale yellow	pale yellow
<i>T</i> (K)	100(2)	100(2)	100(2)	100(2)	100(2)	100(2)
wavelength (Å)	0.71073	0.71073	0.71073	0.71073	0.71073	0.71073
cryst syst	monoclinic	orthorhombic	monoclinic	monoclinic	triclinic	triclinic
space group	<i>P</i> 2 ₁ / <i>c</i>	<i>Pna</i> 2 ₁	<i>P</i> 2 ₁ / <i>c</i>	<i>P</i> 2 ₁ / <i>c</i>	<i>P</i> $\bar{1}$	<i>P</i> $\bar{1}$
<i>a</i> (Å)	17.0102(6)	18.2731(8)	16.9997(9)	14.0277(10)	9.6416(4)	9.9727(7)
<i>b</i> (Å)	9.5281(3)	17.5230(8)	9.6556(5)	11.7222(8)	11.0933(5)	10.4488(7)
<i>c</i> (Å)	19.0872(7)	6.9254(3)	18.9784(10)	26.5468(19)	12.6741(6)	15.4665(13)
α (deg)	90	90	90	90	99.4450(10)	95.4810(10)
β (deg)	115.6030(10)	90	115.7220(10)	95.6880(10)	102.0990(10)	90.6990(10)
γ (deg)	90	90	90	90	96.1810(10)	117.4650(10)
volume (Å ³)	2789.80(17)	2217.51(17)	2806.5(3)	4343.7(5)	1293.24(10)	1420.58(18)
<i>Z</i>	4	4	4	4	2	2
<i>D</i> _{calcd} (Mg/m ³)	1.574	1.665	1.588	1.6	1.506	1.488
abs coeff (mm ⁻¹)	0.801	0.993	0.798	1.379	0.754	0.693
<i>F</i> (000)	1360	1144	1376	2216	604	656
cryst size (mm ³)	0.16 × 0.11 × 0.04	0.46 × 0.05 × 0.03	0.34 × 0.09 × 0.03	0.14 × 0.02 × 0.03	0.25 × 0.22 × 0.03	0.16 × 0.12 × 0.03
θ range (deg)	2.16–27.50	2.23–32.28	2.17–25.99	1.90–27.50	1.67–30.00	2.21–32.35
index ranges	–22 ≤ <i>h</i> ≤ 22 –12 ≤ <i>k</i> ≤ 12 –24 ≤ <i>l</i> ≤ 24	–27 ≤ <i>h</i> ≤ 27 –26 ≤ <i>k</i> ≤ 26 –10 ≤ <i>l</i> ≤ 10	–20 ≤ <i>h</i> ≤ 20 –11 ≤ <i>k</i> ≤ 11 –23 ≤ <i>l</i> ≤ 23	–18 ≤ <i>h</i> ≤ 18 –15 ≤ <i>k</i> ≤ 15 –34 ≤ <i>l</i> ≤ 34	–13 ≤ <i>h</i> ≤ 13 –15 ≤ <i>k</i> ≤ 15 –17 ≤ <i>l</i> ≤ 17	–14 ≤ <i>h</i> ≤ 14 –15 ≤ <i>k</i> ≤ 15 –23 ≤ <i>l</i> ≤ 23
no. of reflns collected	35 712	35 112	31 312	41 651	20 067	25 339
no. of indep reflns	6416	7893	5505	9982	7527	9979
no. of data/restraints/params	<i>R</i> _{int} = 0.0916 6416/0/352	<i>R</i> _{int} = 0.0535 7893/1/271	<i>R</i> _{int} = 0.1148 5505/0/395	<i>R</i> _{int} = 0.2002 9982/0/505	<i>R</i> _{int} = 0.0263 7527/0/352	<i>R</i> _{int} = 0.0622 9979/36/375
GOF on <i>F</i> ²	0.811	1.033	0.983	0.904	1.012	1.004
final <i>R</i> indices	<i>R</i> 1 = 0.0364	<i>R</i> 1 = 0.0345	<i>R</i> 1 = 0.0403	<i>R</i> 1 = 0.0641	<i>R</i> 1 = 0.0288	<i>R</i> 1 = 0.0548
[<i>I</i> > 2 σ (<i>I</i>)]	w <i>R</i> 2 = 0.0721	w <i>R</i> 2 = 0.0729	w <i>R</i> 2 = 0.0866	w <i>R</i> 2 = 0.1045	w <i>R</i> 2 = 0.0695	w <i>R</i> 2 = 0.1228
<i>R</i> indices	<i>R</i> 1 = 0.0663	<i>R</i> 1 = 0.0417	<i>R</i> 1 = 0.0692	<i>R</i> 1 = 0.1542	<i>R</i> 1 = 0.0344	<i>R</i> 1 = 0.0886
(all data)	w <i>R</i> 2 = 0.0759	w <i>R</i> 2 = 0.0761	w <i>R</i> 2 = 0.0934	w <i>R</i> 2 = 0.1221	w <i>R</i> 2 = 0.0714	w <i>R</i> 2 = 0.1378
CCDC no.	616215	616220	616217	616216	616218	616219

solvent was removed under vacuum and the resulting solid extracted with 5 mL of CH_2Cl_2 . Removal of the CH_2Cl_2 under reduced pressure afforded 25 mg (0.04 mmol, 88% yield) of the ruthenium hydride **7** as a pale yellow powder. Alternatively, **7** may be obtained by washing the residue with deoxygenated water to remove the sodium salts. ^1H NMR (400 MHz, $\text{DMSO}-d_6$): δ 7.34–7.19 (m, 15H, Ph); 4.39 (s, 5H Cp); 4.05, 3.82 (AB quartet, $^2J_{\text{HAHB}} = 12.4$ Hz, 6H, NCH_2N); 3.13 (s, 6H, PCH_2N); -13.16 ppm (dd, $^2J_{\text{PH}} = 35.2$ Hz (PTA), 32.4 Hz (PPh_3), 1H, RuH). ^{31}P NMR (162 MHz, $\text{DMSO}-d_6$): δ 68.80 ppm (t, PPh_3 , $^2J_{\text{PP}} = 36.8$ Hz, $^2J_{\text{PH}} = 32.4$ Hz); -23.69 ppm (t, PTA, $^2J_{\text{PP}} = 36.8$ Hz, $^2J_{\text{PH}} = 35.2$ Hz). IR (KBr): $\nu(\text{Ru}-\text{H})$ 1925 cm^{-1} (br). Yellow crystals of $\text{CpRu}(\text{PTA})(\text{PPh}_3)\text{H}$ suitable for X-ray diffraction were obtained by slow evaporation of the solvent from a concentrated methanol solution of **7** at room temperature for 1 h (see Table 1 for details).

Synthesis of $(\eta^5\text{-C}_9\text{H}_7)\text{Ru}(\text{PTA})(\text{PPh}_3)\text{H}$ (8**).** A mixture of $\text{IndRu}(\text{PTA})(\text{PPh}_3)\text{Cl}$ (134 mg, 0.2 mmol) and CH_3ONa (0.2 mmol) was refluxed under nitrogen for 5 h in 40 mL of MeOH. The resulting yellow solution was cooled to room temperature and filtered, and the solvent was removed under vacuum, resulting in 118 mg of **8** as a pale yellow solid (92% yield). ^1H NMR (400 MHz, CD_3OD): δ -16.3 (dd, $^2J_{\text{PTA}-\text{H}} = 32.0$ Hz, $^2J_{\text{PPh}_3-\text{H}} = 29.2$ Hz, 1H, RuH); 4.30 (d, $^2J_{\text{HAHB}} = 12.5$ Hz, 3H, NCH_2N), 4.06 (d, $^2J_{\text{HAHB}} = 12.5$ Hz, 3H, NCH_2N); 4.66 (s, 6H, PCH_2N); δ 7.58–7.13 (m, PPh_3 indenyl, 19H). $^{31}\text{P}\{^1\text{H}\}$ NMR (162 MHz, CD_3OD): δ 62.7 ppm (d, PPh_3 , $^2J_{\text{PP}} = 29.0$ Hz), -23.3 ppm (d, PTA, $^2J_{\text{PP}} = 29.0$ Hz). IR (KBr): $\nu(\text{Ru}-\text{H})$ 1977 cm^{-1} (br). X-ray-quality crystals of $(\eta^5\text{-C}_9\text{H}_7)\text{Ru}(\text{PTA})(\text{PPh}_3)\text{H}$ were grown by slow diffusion of diethyl ether into a methanol solution of **8**.

Transfer Hydrogenation Procedure. The transfer hydrogenation reactions were carried out in a 20 mL Schlenk tube with a Teflon valve. The reactions were conducted in acidic or basic conditions using HCOOH (formic acid), HCOONa (sodium formate), or Na_2CO_3 /isopropanol as the hydrogen source. Each catalytic run was repeated at least twice to ensure reproducibility.

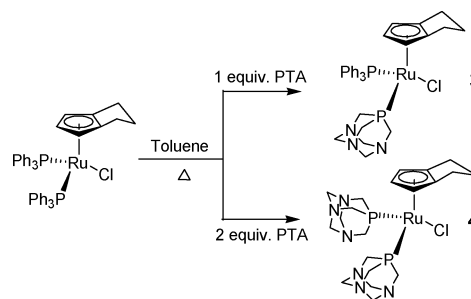
Method A (Acidic Medium). In a typical catalytic run 5 mol % catalyst and the substrate were treated with 40 μL of 88% HCOOH in 2 mL of water. The resultant solution was stirred at 80 $^\circ\text{C}$ in an oil bath. The solution was cooled to room temperature and the product(s) extracted with hexanes (2×3 mL). The hexanes layer was analyzed by GC-MS and ^1H NMR spectroscopy, and the peaks were identified by comparison with authentic samples. Yields were determined by ^1H NMR integrations of all products and remaining starting material.

Method B (Basic Medium). In a typical run, the ruthenium complex, unsaturated carbonyl, and HCOONa in mole ratio of 1:20:500 were dissolved in 2 mL of water or a mixture of water/methanol (2:3 mL). Alternatively the catalyst, substrate, and Na_2CO_3 in 1:20:212 mole ratio were dissolved in 7 mL of water/isopropanol (4:3 mL). The reaction temperature, workup, and analysis are the same as in method A.

Results and Discussion

Preparation of $\text{Cp}'\text{Ru}(\text{PTA})(\text{PR}_3)\text{Cl}$ Complexes, $\text{Cp}' = \text{Cp, Dp, Ind}$; $\text{PR}_3 = \text{PTA}$ or PPh_3 . The synthesis of a series of half-sandwich Ru(II) complexes, of the type $\text{Cp}'\text{Ru}(\text{PTA})(\text{PR}_3)\text{Cl}$, $\text{Cp}' = \text{Cp, Dp, Ind}$; $\text{PR}_3 = \text{PTA}$ or PPh_3 , was accomplished in good to excellent yields. The complexes $\text{CpRu}(\text{PTA})_2\text{Cl}^{14,16}$ and $\text{CpRu}(\text{PTA})(\text{PPh}_3)\text{Cl}^{25}$ have been previously synthesized by addition of PTA to $\text{CpRu}(\text{PPh}_3)_2\text{Cl}$ in toluene. In our hands, the reaction of PTA with $\text{CpRu}(\text{PPh}_3)_2\text{Cl}$ in refluxing toluene afforded the monosubstituted complex $\text{CpRu}(\text{PTA})(\text{PPh}_3)\text{Cl}$ (**1**) in low yield and the disubstituted complex $\text{CpRu}(\text{PTA})_2\text{Cl}$ (**2**) in high yield as a precipitate irrespective of the stoichiometric proportions of the reactants. This observation is consistent with that described for the reaction of $\text{CpRu}(\text{PPh}_3)_2\text{-}$

Scheme 1



Scheme 2

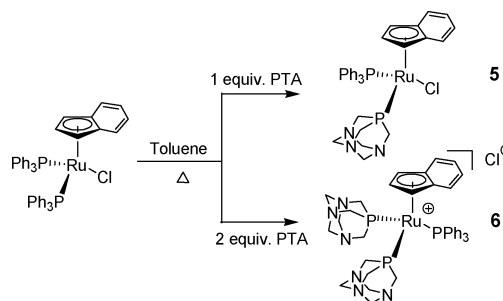


Table 2. $^{31}\text{P}\{^1\text{H}\}$ Chemical Shifts and Coupling Constants for the Series of $\text{Cp}'\text{Ru}(\text{PTA})(\text{PR}_3)\text{Cl}$ Complexes ($\text{Cp}' = \text{Cp, Dp, Ind}$; $\text{PR}_3 = \text{PTA}$ or PPh_3) in CDCl_3

complex	$^{31}\text{P}\{^1\text{H}\}$ NMR	$^2J_{\text{PP}}$, Hz
$\text{CpRu}(\text{PPh}_3)_2\text{Cl}$	40.15	
$\text{CpRu}(\text{PTA})(\text{PPh}_3)\text{Cl}$ (1)	48.4 (PPh_3) -34.5 (PTA)	45.0
$\text{CpRu}(\text{PTA})_2\text{Cl}$ (2) ^{a,14,16}	-25.65	
$\text{DpRu}(\text{PPh}_3)_2\text{Cl}$ ^{b,19}	41.4	
$\text{DpRu}(\text{PTA})(\text{PPh}_3)\text{Cl}$ (3)	43.2 (PPh_3) -39.6 (PTA)	45.2
$\text{DpRu}(\text{PTA})_2\text{Cl}$ (4)	-27.3	
$\text{IndRu}(\text{PPh}_3)_2\text{Cl}$ ²³	47.4	
$\text{IndRu}(\text{PTA})(\text{PPh}_3)\text{Cl}$ (5)	50.8 (PPh_3) -22.6 (PTA)	42.8
$[\text{IndRu}(\text{PTA})_2(\text{PPh}_3)]\text{Cl}$ (6)	48.9 (PPh_3) -34.1 (PTA)	30.1

^a In CD_2Cl_2 . ^b In C_6D_6 .

Cl with aminophosphines, Ph_2PNHR ($\text{R} = \text{Ph, C}_6\text{H}_{11}$).²⁶ We have obtained $\text{CpRu}(\text{PTA})(\text{PPh}_3)\text{Cl}$ cleanly in modest yield (62%) by stirring equimolar amounts of PTA and $\text{CpRu}(\text{PPh}_3)_2\text{-Cl}$ in CH_2Cl_2 at room temperature for 14 h. $\text{Cp}'\text{Ru}(\text{PTA})(\text{PPh}_3)\text{-Cl}$, $\text{Cp}' = \eta^5\text{-C}_8\text{H}_9$ (**3**) or $\eta^5\text{-C}_9\text{H}_7$ (**5**), complexes were prepared by refluxing equimolar amounts of PTA and $\text{Cp}'\text{Ru}(\text{PPh}_3)_2\text{Cl}$ in toluene, affording **3** in 50% yield and **5** in 72% yield. The bis-PTA complex $\text{DpRu}(\text{PTA})_2\text{Cl}$ (**4**) was obtained as a yellow precipitate in >98% yield by refluxing a toluene solution of PTA (0.5 mmol) and $\text{DpRu}(\text{PPh}_3)_2\text{Cl}$ (0.23 mmol) for 3 h, Scheme 1. Attempts to synthesize $\text{IndRu}(\text{PTA})_2\text{Cl}$ in an analogous manner resulted in the formation of the cationic species $[\text{IndRu}(\text{PTA})_2(\text{PPh}_3)]\text{Cl}$ (**6**) in 89% yield, Scheme 2.

The spectroscopic data for compounds **3–6** support the formulation of the complexes²⁷ and were confirmed by X-ray crystallography (*vide infra*). The $^{31}\text{P}\{^1\text{H}\}$ NMR spectra of the $\text{Cp}'\text{Ru}(\text{PTA})(\text{PPh}_3)\text{Cl}$ complexes each consist of two doublets due to coupling of the inequivalent phosphorus nuclei: $^2J_{\text{PP}} = 45.0$ Hz, **1**; 45.2 Hz, **3**; 42.8 Hz, **5**; Table 2. The indenyl complex $[\text{IndRu}(\text{PTA})_2(\text{PPh}_3)]\text{Cl}$ also exhibits two sets of resonances in

(26) Priya, S.; Balakrishna, M. A.; Mobin, S. M.; McDonald, R. J. *Organomet. Chem.* **2003**, 688, 227–235.

(27) See Supporting Information for details.

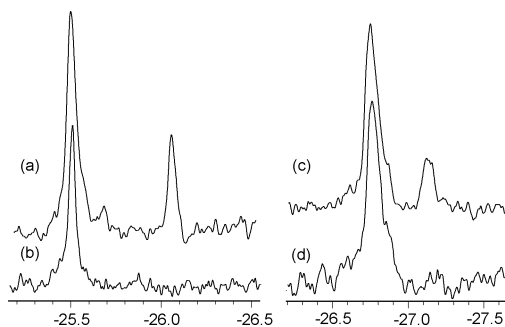
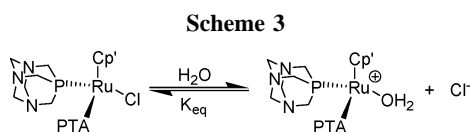


Figure 1. $^{31}\text{P}\{^1\text{H}\}$ NMR spectra of **2** and **4** in D_2O : (a) $\text{CpRu}(\text{PTA})_2\text{Cl}$ (-25.50 ppm) and $[\text{CpRu}(\text{PTA})_2(\text{OH}_2)]^+$ (-26.05 ppm); (b) in 0.027 M KCl only $\text{CpRu}(\text{PTA})_2\text{Cl}$ is observed; (c) $\text{DpRu}(\text{PTA})_2\text{Cl}$ (-26.76 ppm) and $[\text{DpRu}(\text{PTA})_2(\text{OH}_2)]^+$ (-27.15 ppm); (d) in 0.027 M KCl only $\text{DpRu}(\text{PTA})_2\text{Cl}$ is observed.



the $^{31}\text{P}\{^1\text{H}\}$ NMR spectrum; 48.9 (t, PPh_3 , $^2J_{\text{PP}} = 30.1$ Hz) and -34.1 ppm (d, PTA, $^2J_{\text{PP}} = 30.1$ Hz). The $^{31}\text{P}\{^1\text{H}\}$ NMR spectrum of $\text{DpRu}(\text{PTA})_2\text{Cl}$ (**4**) in CDCl_3 contains a single resonance at -27.3 ppm corresponding to an ~ 2 ppm downfield shift from $\text{CpRu}(\text{PTA})_2\text{Cl}$ ^{14,16} and an ~ 7 ppm upfield shift from the Cp^* analogue, $\text{Cp}^*\text{Ru}(\text{PTA})_2\text{Cl}$ (-34.23 ppm).¹⁶ The ^1H NMR spectrum of **4** exhibits a classic AB pattern for the NCH_2N protons of PTA centered at 4.51 and 4.59 ppm; the PCH_2N and C_5H_3 resonances overlap between 4.00 – 4.17 ppm. A set of broad multiplets were observed for the $\text{Cp}(\text{CH}_2)_3$ protons between 2.50 and 1.96 ppm.

The bis-PTA complexes, $\text{CpRu}(\text{PTA})_2\text{Cl}$ (**2**) and $\text{DpRu}(\text{PTA})_2\text{Cl}$ (**4**), are soluble in aqueous solution; $S_{25^\circ\text{C}} = 40$ mg/mL¹⁶ and $S_{25^\circ\text{C}} = 43$ mg/mL, respectively. ^1H and $^{31}\text{P}\{^1\text{H}\}$ NMR spectra of **2** and **4** in aqueous solution both contain two sets of resonances (Figure 1), the relative heights of which are concentration-dependent: ^{31}P NMR (D_2O): **2**, δ -25.50 and -26.05 ppm; **4**, δ -26.76 and -27.15 ppm. The two resonances observed in aqueous solution indicate the existence of two species presumably due to the partial hydrolysis of the ruthenium–chloride bond and the formation of the corresponding aqua complex, Scheme 3. The solid-state structures of two $[\text{CpRu}(\text{PR}_3)_2(\text{OH}_2)]^+$ cations have been reported: a water-soluble silver containing polymer of $[\text{CpRu}(\text{PTA})_2(\text{OH}_2)]^+$ ²⁸ and an alkyne hydration catalyst $[\text{CpRu}(\text{PPh}_2\text{Ar})_2(\text{OH}_2)]^+$ (where $\text{Ar} = 4$ -*tert*-butyl-*N*-methylimidazole).²⁹ As depicted in Scheme 3, the chloride and aqua complexes are in equilibrium; addition of Cl^- shifts the equilibrium to the left, decreasing the concentration of the aqua complex ($K_{\text{eq}} = 6.18 \times 10^{-4}$ for **2** and 5.08×10^{-4} for **4**).

The mixed phosphine complex **1** is insoluble in water ($S_{25^\circ\text{C}} = 1.5$ mg/mL),²⁵ as are compounds **3** and **5**. In acidic solutions; however, complexes **1** and **3** become soluble in aqueous solution, presumably due to protonation of the PTA ligand, affording the cationic species $[\text{Cp}'\text{Ru}(\text{PTAH})(\text{PPh}_3)\text{Cl}]^+$, $\text{Cp}' = \text{Cp}$ (**1H**⁺), Dp (**3H**⁺). The formation of $[\text{Cp}'\text{Ru}(\text{PTAH})(\text{PPh}_3)\text{Cl}]^+$ was observed, by $^{31}\text{P}\{^1\text{H}\}$ NMR spectroscopy. Treatment of $\text{Cp}'\text{Ru}(\text{PTA})(\text{PPh}_3)\text{Cl}$ with HCO_2H in water ($\text{pH} \leq 3$) resulted in a substantial shift in the $^{31}\text{P}\{^1\text{H}\}$ NMR spectrum

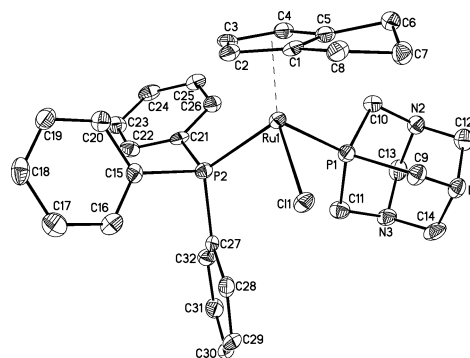


Figure 2. Thermal ellipsoid (50% probability) representation of $\text{DpRu}(\text{PTA})(\text{PPh}_3)\text{Cl}$ (**3**) with the atomic numbering scheme.

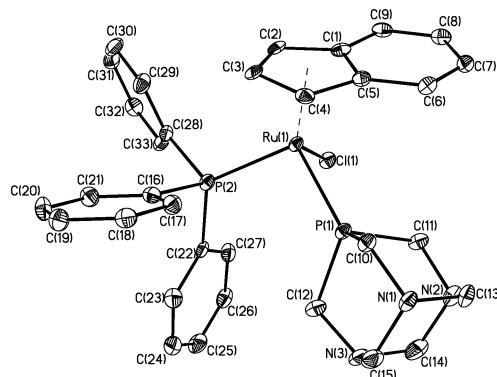


Figure 3. Thermal ellipsoid (50% probability) representation of $\text{IndRu}(\text{PTA})(\text{PPh}_3)\text{Cl}$ (**5**) with the atomic numbering scheme.

consistent with protonation of a PTA ligand (-10.59 ppm, d, PTAH , $^2J_{\text{PP}} = 16$ Hz, **1H**⁺; -7.77 ppm, br, PTAH , **3H**⁺) and a very small shift in the PPh_3 resonance (55.34 ppm, d, PPh_3 , $^2J_{\text{PP}} = 16$ Hz, **1H**⁺; 59.60 ppm, br, PPh_3 , **3H**⁺). The mixed phosphine indenyl complex **5** is essentially insoluble even in acidic solution. As observed for compound **2**,¹³ $\text{DpRu}(\text{PTA})_2\text{Cl}$ can be protonated at a PTA nitrogen to afford $[\text{DpRu}(\text{PTAH})_2\text{Cl}]^{2+}$ or $[\text{DpRu}(\text{PTAH})(\text{PTA})\text{Cl}]^+$. Protonation results in a shift in the $^{31}\text{P}\{^1\text{H}\}$ NMR spectrum of 9.6 ppm to -17.71 ppm, similar in magnitude to the chemical shift difference between $\text{CpRu}(\text{PTA})_2\text{Cl}$ and $[\text{CpRu}(\text{PTAH})_2\text{Cl}]^{2+}$ ($\Delta = 10.05$ ppm).¹³

Structure of $\text{Cp}'\text{Ru}(\text{PTA})(\text{PR}_3)\text{Cl}$ Complexes, $\text{Cp}' = \text{Dp}$, **Ind; $\text{PR}_3 = \text{PTA}$ or PPh_3 .** Thermal ellipsoid representations of the solid-state structures of $\text{DpRu}(\text{PTA})(\text{PPh}_3)\text{Cl}$ (**3**) and $\text{IndRu}(\text{PTA})(\text{PPh}_3)\text{Cl}$ (**5**), along with the atomic numbering schemes, are depicted in Figures 2 and 3, respectively. The structure of $\text{CpRu}(\text{PTA})(\text{PPh}_3)\text{Cl}$ was recently reported;²⁵ however, we report here a different crystal morphology resulting in slightly different bond lengths and angles.²⁷ Orange plates of $\text{DpRu}(\text{PTA})(\text{PPh}_3)\text{Cl}$ suitable for X-ray diffraction were obtained by slow evaporation of a toluene solution. X-ray-quality crystals of $\text{IndRu}(\text{PTA})(\text{PPh}_3)\text{Cl}$ were obtained as orange-red rods by slow diffusion of diethyl ether into a dichloromethane solution of the complex. All three piano stool complexes, $\text{Cp}'\text{Ru}(\text{PTA})(\text{PPh}_3)\text{Cl}$ ($\text{Cp}' = \text{Cp}$, Dp , Ind), consist of an η^5 - Cp' ligand bound to ruthenium along with one PTA, one PPh_3 , and a chloride ligand. The $\text{Ru}-\text{Cl}$ distances are comparable and observed to be between 2.445 and 2.466 Å, Table 3. The $\text{Ru}-\text{P}$ distances vary between 2.247 and 2.314 Å for the series depending on the phosphine and ancillary Cp' ligand. A slight increase in the $\text{P1}-\text{Ru}-\text{P2}$ bond angle is observed as the Cp' ligand changes: Cp $95.39(4)$; Dp $97.80(3)$; Ind $98.19(4)$. The $\text{Cp}-\text{ML}_2$ angle between the plane defined by the Cp' ligand and the plane

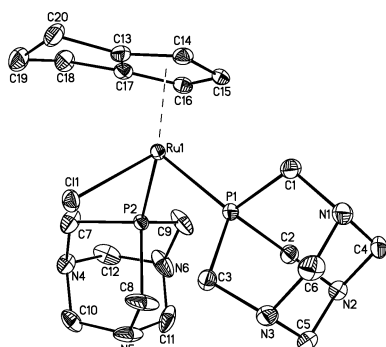
(28) Lidrissi, C.; Romerosa, A.; Saoud, M.; Serrano-Ruiz, M.; Gonsalvi, L.; Peruzzini, M. *Angew. Chem., Int. Ed.* **2005**, *44*, 2568–2572.

(29) Grotjahn, D. B.; Incarvito, C. D.; Rheingold, A. L. *Angew. Chem., Int. Ed.* **2001**, *40*, 3884–3887.

Table 3. Selected Bond Lengths [Å] and Angles [deg] for a Series of Cp'Ru(PTA)(PR₃)Cl Complexes; Cp' = Cp, Dp, or Ind; and PR₃ = PTA or PPh₃

	CpRu(PTA)(PPh ₃)Cl ^a (1)	CpRu(PTA) ₂ Cl ¹⁴ (2)	DpRu(PTA)(PPh ₃)Cl (3)	DpRu(PTA) ₂ Cl (4)	IndRu(PTA)(PPh ₃)Cl (5)
Ru–Cl	2.4664(10)	2.445(2)	2.4529(8)	2.4523(7)	2.4465(9)
Ru–P1	2.3139(11)	2.258(3)	2.2923(9)	2.2645(7)	2.2931(10)
Ru–P2	2.3041(11)	2.247(3)	2.3089(9)	2.2571(7)	2.2697(10)
Ru–Cp' _{cent}	1.861	1.846	1.842	1.855	1.890
P1–Ru–P2	95.39(4)	96.85(5)	97.80(3)	93.20(2)	98.19(4)
P1–Ru–Cl	90.27(3)	91.61(7)	88.06(3)	89.83(2)	90.03(3)
P2–Ru–Cl	91.68(3)	86.46(7)	93.57(3)	87.03(2)	91.99(3)
Cp–ML ₂	51.9	55.3	54.3	54.2	51.4

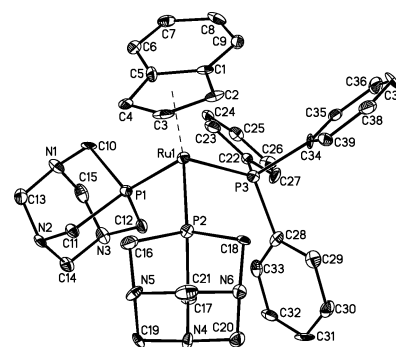
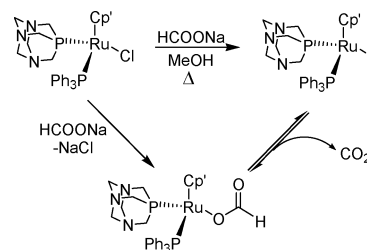
^a See Supporting Information for the crystallographic details and ref 25 for a different polymorph of this compound.

**Figure 4.** Thermal ellipsoid (50% probability) representation of DpRu(PTA)₂Cl (**4**) with the atomic numbering scheme.

defined by P1–Ru1–P2 varies slightly between the Cp, Dp, and Ind complexes (Table 3). The distance between the Ru and the Cp' plane (Cp_{cent}) is observed between 1.84 and 1.89 Å, consistent with standard Ru–Cp' distances.

Yellow needles of **4** suitable for X-ray diffraction were obtained by slow diffusion of diethyl ether into a dichloromethane solution of DpRu(PTA)₂Cl. A thermal ellipsoid representation is depicted in Figure 4 showing the piano stool geometry of **4** with two PTA ligands, a chloride, and an η⁵-coordinated C₈H₉[–] ancillary ligand. The PTA ligands are bound through the phosphorus as expected, with a P–Ru–P bond angle of 93.20(2)°, slightly smaller than that reported for the Cp analogue (96.85(5)°)¹⁴ and similar to that reported for Cp*Ru(PTA)₂Cl (93.30(5)°).¹⁶ This suggests that Cp* and Dp ligands may have similar stereoelectronic influence on the metal center. The Ru–P (2.264, 2.257 Å), Ru–Cl (2.452 Å), and Ru–Cp_{cent} (1.855 Å) distances for **4** are comparable to those of the Cp and Cp* analogues, Table 3.^{14,16} The saturated portion of the η⁵-C₈H₉ (Dp) ligand of **4** has an endo-conformation with an envelope angle of 28.4°, defined as the dihedral angle between the C₅H₃ plane and that of C18–C19–C20, slightly larger than that reported for DpRu(PPh₃)₂Cl (26.4°).¹⁹ The envelope angle in DpRu(PTA)(PPh₃)Cl was found to be 29.5°, larger than that observed for either DpRu(PPh₃)₂Cl or **4**. The (N)C–N distances for the triazacyclohexane ring of the PTA ligands in complexes **1–5** are consistent with nonprotonated PTA ligands (N–C(N) = 1.447–1.480 Å).³⁰

Structure of [IndRu(PTA)₂(PPh₃)](SnCl₃). Due to difficulties related to crystal growth of [IndRu(PTA)₂(PPh₃)]Cl (**6**), [IndRu(PTA)₂(PPh₃)](SnCl₃) was synthesized by stirring a mixture of [IndRu(PTA)₂(PPh₃)]Cl with an excess of SnCl₂·2H₂O. Spectroscopically, both **6** and [IndRu(PTA)₂(PPh₃)](SnCl₃) are identical; the ³¹P{¹H} NMR spectra of both compounds contain

**Figure 5.** Thermal ellipsoid (50% probability) representation of the cation of [IndRu(PTA)₂(PPh₃)](SnCl₃) along with the atomic numbering scheme. Selected bond lengths (Å) and angles (deg): Ru1–P1 = 2.3076(19); Ru1–P2 = 2.2576(18); Ru1–P3 = 2.3456(19); Ru1–Ind_{cent} = 1.936; P1–Ru1–P2 = 92.99(7); P1–Ru1–P3 = 97.47(7); P2–Ru1–P3 = 95.56(7).**Scheme 4**

a triplet at 48.9 ppm (²J_{PP} = 30.1 Hz) for the PPh₃ ligand and a doublet at –34.1 ppm (²J_{PP} = 30.1 Hz) for the two PTA ligands. A thermal ellipsoid representation of the structure of [IndRu(PTA)₂(PPh₃)](SnCl₃) may be found in Figure 5 along with the atomic numbering scheme and selected bond lengths and angles. The structure is not unusual, with the indenyl ligand bound to ruthenium in a η⁵-fashion and the two PTA ligands and one PPh₃ bound in a classic piano stool fashion about the metal. It is interesting that the two PTA ligands are not equivalent, with one Ru–P_{PTA} distance significantly shorter: Ru–P_{PTA} = 2.3076(19) and 2.2576(18) Å. The triphenylphosphine ligand exhibits the longest Ru–P bond length at 2.3456(19) Å, Ru–P3. A complete listing of bond lengths and angles may be found in the Supporting Information.

Cp'Ru(PTA)(PPh₃)H Complexes (Cp' = Cp, Dp, Ind): Synthesis and Reactivity. The air-sensitive ruthenium hydrides, Cp'Ru(PTA)(PPh₃)H (Cp' = Cp, In), were obtained in good yield by the reaction of Cp'Ru(PTA)(PPh₃)Cl with sodium formate or sodium methoxide in refluxing methanol, Scheme 4. The ¹H NMR spectra show characteristic Ru–H resonances at –13.2 ppm (²J_{PTA–H} = 36.0 Hz, ²J_{PPh₃–H} = 33.0 Hz) for **7** and at –16.3 ppm (²J_{PTA–H} = 32.0 Hz, ²J_{PPh₃–H} = 29.2 Hz) for **8**. Table 4 contains detailed ³¹P{¹H} data on the series of

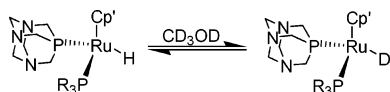
(30) Daresbourg, D. J.; Decuir, T. J.; Reibenspies, J. H. *Aqueous Organometallic Chemistry and Catalysis*; Horvath, I. T., Joó, F., Eds.; NATO ASI Ser., Ser. 3; High Technology; Kluwer: Dordrecht, The Netherlands, 1995; pp 61–80.

Table 4. $^{31}\text{P}\{^1\text{H}\}$ NMR Chemical Shifts and Coupling Constants for a Series of $\text{Cp}'\text{Ru}(\text{PTA})(\text{PPh}_3)\text{H}$ and $\text{Cp}'\text{Ru}(\text{PTA})_2\text{H}$ Complexes ($\text{Cp}' = \text{Cp}, \text{Dp}, \text{Ind}$)

complex	chemical shift, ppm	$^2J_{\text{PP}}$, Hz	$^2J_{\text{PH}}$, Hz
$\text{CpRu}(\text{PTA})_2\text{H}^{14,a}$	-12.0		36.6
$\text{CpRu}(\text{PTA})(\text{PPh}_3)\text{H}$ (7) ^b	68.80 (PPh ₃) -23.69 (PTA)	36.8	32.4 (PPh ₃) 35.2 (PTA)
$\text{CpRu}(\text{PPh}_3)_2\text{H}^b$	67.76		33.2
$\text{IndRu}(\text{PTA})(\text{PPh}_3)\text{H}$ (8) ^c	62.7 (PPh ₃) -23.3 (PTA)	29.0	29.2 (PPh ₃) 32.0 (PTA)
$\text{IndRu}(\text{PPh}_3)_2\text{H}^{23}$	64.5		33.9
$\text{DpRu}(\text{PTA})_2\text{H}^b$	-17.8		36.0
$\text{DpRu}(\text{PTA})(\text{PPh}_3)\text{H}^b$	68.39 (PPh ₃) -25.90 (PTA)	37.0	32.0 (PPh ₃) 36.0 (PTA)

^a In D₂O. ^b In DMSO-*d*₆. ^c In CD₃OD.

Scheme 5. H/D Exchange between $\text{Cp}'\text{Ru}(\text{PTA})(\text{PR}_3)\text{H}$ and CD_3OD ; $\text{Cp}' = \eta^5\text{-(C}_5\text{H}_5\text{)}, \eta^5\text{-(C}_9\text{H}_7\text{)}, \text{ or } \eta^5\text{-(C}_8\text{H}_9\text{)}$ and $\text{PR}_3 = \text{PTA or PPh}_3$



Ru-H complexes. The $^{31}\text{P}\{^1\text{H}\}$ spectrum of $\text{CpRu}(\text{PTA})(\text{PPh}_3)\text{H}$ recorded in DMSO-*d*₆ contained resonances at 68.80 ppm (d, PPh₃, $^2J_{\text{PP}} = 36.8$ Hz) and -23.69 ppm (d, PTA, $^2J_{\text{PP}} = 36.8$ Hz). The $^{31}\text{P}\{^1\text{H}\}$ NMR spectrum of $\text{IndRu}(\text{PTA})(\text{PPh}_3)\text{H}$ in CD₃OD contained signals at 62.7 ppm (d, PPh₃) and -23.3 ppm (d, PTA), $^2J_{\text{PP}} = 29.0$ Hz. The preparation of $\text{DpRu}(\text{PTA})(\text{PR}_3)\text{H}$ ($\text{PR}_3 = \text{PTA or PPh}_3$) via analogous methods leads to the formation of the respective Ru-H complex along with an unidentified species and is still under investigation. Preliminary ^1H NMR spectroscopic results in DMSO-*d*₆ reveal the Ru-H resonances for $\text{DpRu}(\text{PTA})_2\text{H}$ at $\delta -14.13$ ppm (t, $^2J_{\text{PH}} = 36.0$ Hz) and at $\delta -12.88$ ppm (t, $^2J_{\text{PPh}_3\text{-H}} = 32.0$ Hz, $^2J_{\text{PTA-H}} = 36.0$ Hz) for $\text{DpRu}(\text{PTA})(\text{PPh}_3)\text{H}$.

We have previously reported that $\text{CpRu}(\text{PTA})_2\text{H}$ undergoes H/D exchange with D₂O, $t_{1/2} = 127$ min at 25 °C; in CD₃OD no H/D exchange was observed over the course of weeks at room temperature.¹⁴ Interestingly, $\text{CpRu}(\text{PTA})(\text{PPh}_3)\text{H}$ undergoes rapid H/D exchange ($t_{1/2} \ll 10$ min) with CD₃OD, affording $\text{CpRu}(\text{PTA})(\text{PPh}_3)\text{D}$; however, much slower H/D exchange ($t_{1/2} \approx 5.5$ days, $k_{\text{obs}} \approx 0.12 \text{ day}^{-1}$) was observed for $\text{IndRu}(\text{PTA})(\text{PPh}_3)\text{H}$ in CD₃OD at 25 °C (Scheme 5). Electronic differences alone between $\text{CpRu}(\text{PTA})(\text{PPh}_3)\text{H}$ and $\text{IndRu}(\text{PTA})(\text{PPh}_3)\text{H}$ are not likely responsible for this difference.³¹ The formation of $\text{Cp}'\text{Ru}(\text{PTA})(\text{PPh}_3)\text{D}$ was confirmed by the disappearance of the hydride resonance in the ^1H NMR spectrum, a slight isotopic shift, and a change in the splitting of the $^{31}\text{P}\{^1\text{H}\}$ NMR resonances, and by IR spectroscopy. The $\nu(\text{Ru-H})$ of $\text{IndRu}(\text{PTA})(\text{PPh}_3)\text{H}$, $\text{CpRu}(\text{PTA})(\text{PPh}_3)\text{H}$, and $\text{DpRu}(\text{PTA})(\text{PPh}_3)\text{H}$ varies a great deal with the electronic nature of the Cp' ligand ($\text{Ind} > \text{Cp} > \text{Dp}$): $\nu(\text{Ru-H}) = 1977, 1925, \text{ and } 1898 \text{ cm}^{-1}$ respectively. Isotopic labeling has been used to identify the IR bands as $\nu(\text{Ru-H})$; deuteration of **7** results in the disappearance of the absorption band at 1925 cm^{-1} and appearance of a new absorbance at 1385 cm^{-1} for $\text{CpRu}(\text{PTA})(\text{PPh}_3)\text{D}$ assigned to the $\nu(\text{Ru-D})$ stretch. The observed isotopic shift (540 cm^{-1} for **7**) is close to the calculated value based on Hooke's law (554 cm^{-1}).³²

(31) The details of this unexpectedly large variation in the rate of H/D exchange in the Cp and Ind complexes are currently under further investigation; a change in mechanism or possibly an acidic impurity may be involved.

(32) Drago, R. S. *Physical Methods for Chemists*, 2nd ed.; Saunders: Philadelphia, 1992.

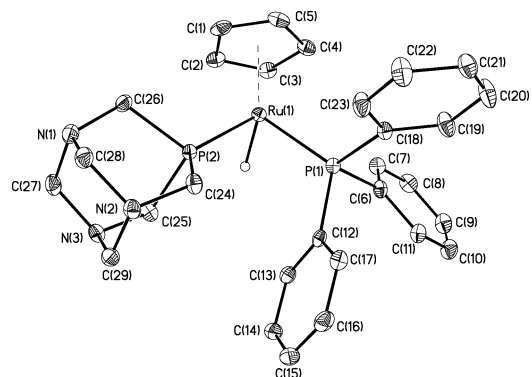


Figure 6. Thermal ellipsoid (50% probability) representation of $\text{CpRu}(\text{PTA})(\text{PPh}_3)\text{H}$ (**7**) with the atomic numbering scheme.

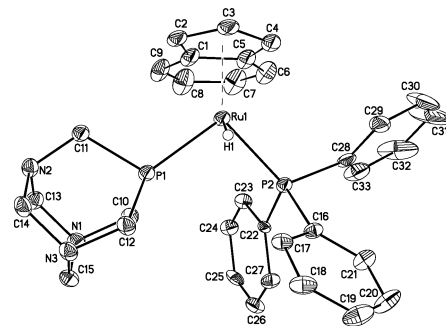


Figure 7. Thermal ellipsoid (50% probability) representation of $\text{IndRu}(\text{PTA})(\text{PPh}_3)\text{H}$ (**8**) with the atomic numbering scheme.

Table 5. Selected Bond Lengths [Å] and Angles [deg] for $\text{CpRu}(\text{PTA})(\text{PPh}_3)\text{H}$ (**7**) and $\text{IndRu}(\text{PTA})(\text{PPh}_3)\text{H}$ (**8**)

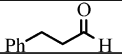
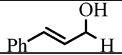
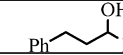
	$\text{IndRu}(\text{PTA})(\text{PPh}_3)\text{H}$	$\text{CpRu}(\text{PTA})(\text{PPh}_3)\text{H}$
Ru-H	1.52(4)	1.53(2)
Ru-P1	2.2564(8)	2.2543(4)
Ru-P2	2.2539(8)	2.2449(4)
$\text{Ru-Cp}'_{\text{cent}}$	1.929	1.894
P1-Ru-P2	97.59(3)	97.703(16)
P1-Ru-H	83.1(15)	81.4(8)
P2-Ru-H	82.7(15)	81.6(8)
Cp-ML_2	69.9	72.7

Solid-State Structure of $\text{CpRu}(\text{PTA})(\text{PPh}_3)\text{H}$ (7**) and $\text{IndRu}(\text{PTA})(\text{PPh}_3)\text{H}$ (**8**).** Single-crystal X-ray diffraction was performed on suitable crystals of $\text{CpRu}(\text{PTA})(\text{PPh}_3)\text{H}$ (**7**) and $\text{IndRu}(\text{PTA})(\text{PPh}_3)\text{H}$ (**8**), Table 1. Both sets of crystals were grown by slow evaporation of a concentrated methanol solution of the Ru-H . Thermal ellipsoid plots of **7** and **8** are presented in Figures 6 and 7, respectively; along with the atomic numbering scheme, selected bond lengths and angles may be found in Table 5. The structures of the $\text{Cp}'\text{Ru}(\text{PTA})(\text{PPh}_3)\text{H}$ complexes are similar to those of the parent Ru-Cl complexes with the notable difference of a significant increase in the Cp-ML_2 angle as the chloride ligand is replaced by the much smaller and electronically different hydride. The Cp-ML_2 angle was found to be 72.7° and 69.9° , respectively, for **7** and **8**, which compares favorably with the value of 67.8° reported by us for the $\text{CpRu}(\text{PTA})_2\text{H}$ complex.¹⁴ This is $\sim 20^\circ$ larger than the values reported for compounds **1** and **5** and consistent with the mean value of 67.6° reported for a series of $\text{Cp}'\text{M}(\text{L}_2)\text{H}$ complexes.³³ The change in Cp-ML_2 angle from the Ru-Cl to the Ru-H complexes can be ascribed to both an electronic effect and the smaller steric requirement of H^- versus Cl^- .

Transfer Hydrogenation of α,β -Unsaturated Substrates. Selective transfer hydrogenation of α,β -unsaturated carbonyls

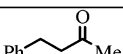
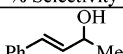
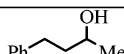
(33) Lemke, F. R.; Brammer, L. *Organometallics* **1995**, *14*, 3980-3987.

Table 6. Selective Transfer Hydrogenation of Cinnamaldehyde by Complexes 1–5 and 7 with HCOOH or HCOONa as Hydrogen Donor^f

Entry	Catalyst	%Con.	TOF (h ⁻¹)	% Selectivity		
						
1	CpRu(PTA)(PPh ₃)Cl	>99.0	3.3	0.0	80.3	19.7
2 ^a	CpRu(PTA)(PPh ₃)Cl	>99.0	3.3	0.0	<1.0	>99.0
3 ^a	CpRu(PTA)(PPh ₃)H	>99.0	3.3	0.0	0.0	>99.0
4	CpRu(PTA) ₂ Cl	89.5	2.8	0.0	<1.0	>99.0
5 ^b	CpRu(PTA) ₂ Cl	69.6	2.3	48.1	0.0	51.9
6 ^c	CpRu(PTA) ₂ Cl	11.1	1.5	85.6	7.2	7.2
7	DpRu(PTA)(PPh ₃)Cl	>99.0	3.5	0.0	78.2	21.8
8	DpRu(PTA) ₂ Cl	>99.0	3.5	0.0	100.0	0.0
9 ^b	DpRu(PTA) ₂ Cl	>99.0	3.5	0.0	0.0	100.0
10 ^d	IndRu(PTA)(PPh ₃)Cl	>99.0	0.83	0.0	54.8	45.2
11 ^e	-----	0.0	0.0	-	-	-

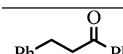
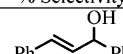
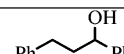
^a 100 μ L of 88% HCOOH. ^b 0.9 mmol (61.2 mg) of HCO₂Na used in lieu of HCO₂H, pH \approx 9. ^c 2 mmol of cinnamaldehyde, 0.03 mmol of catalyst, 22 mmol of HCO₂Na, 6 mL of H₂O, 80 $^{\circ}$ C, 5 h.¹⁵ ^d 5 mol % of catalyst, 3.7–4.0 μ L of cinnamaldehyde, 150 μ L of 88% HCOOH, 2 mL of H₂O, 1 mL of MeOH, 24 h. ^e No catalyst, 4.0 μ L of cinnamaldehyde, 60 μ L of HCO₂H, 80 $^{\circ}$ C, 12 h. ^f General conditions: 5 mol % of catalyst, 4.0–4.5 μ L of cinnamaldehyde, 40 μ L of 88% HCO₂H, 2 mL of H₂O, 6 h, 80 $^{\circ}$ C, pH \approx 3.

Table 7. Selective Transfer Hydrogenation of Benzylidene Acetone by 1–5 and 7 Using HCOOH or HCOONa as the Reducing Agent^e

Entry	Catalyst	% Con.	TOF (h ⁻¹)	% Selectivity		
						
1	CpRu(PTA)(PPh ₃)Cl	79.4	0.7	55.9	0.0	34.7
2	CpRu(PTA) ₂ Cl	66.7	0.6	100.0	0.0	0.0
3 ^{a,b}	CpRu(PTA) ₂ Cl	78.9	0.6	>99.0	<1.0	0.0
4 ^{c,d}	CpRu(PTA) ₂ Cl	36.1	6.0	93.9	6.1	0.0
5 ^c	DpRu(PTA)(PPh ₃)Cl	51.1	1.7	100	0.0	0.0
6	DpRu(PTA) ₂ Cl	81.4	0.8	58.7	41.3	0.0
7 ^a	DpRu(PTA) ₂ Cl	83.7	0.8	100.0	0.0	0.0
8 ^c	IndRu(PTA)(PPh ₃)Cl	48.9	0.41	100.0	0.0	0.0
9 ^f	CpRu(PTA)(PPh ₃)H	38.5	0.64	100.0	0.0	0.0

^a 0.9 mmol (61.2 mg) of HCO₂Na in lieu of HCO₂H, pH \approx 9. ^b 25 h. ^c 6 h. ^d 0.75 mmol of substrate, 7.5 \times 10⁻³ mmol of catalyst, 7.5 mmol of HCO₂Na, 3 mL of MeOH, 3 mL of H₂O, 90 $^{\circ}$ C, 6 h.¹⁵ ^e 150 μ L of HCOOH, 2 mL of H₂O, 1 mL of MeOH. ^f 100 μ L of HCOOH, 12 h. ^g General conditions: 5 mol % of catalyst; 4.3 mg of benzylidene acetone; 40 μ L of 88% HCO₂H; 2 mL of H₂O; 24 h at 80 $^{\circ}$ C; pH \approx 3.

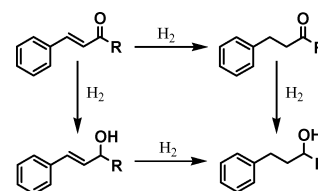
Table 8. Selective Transfer Hydrogenation of Chalcone by Compounds 1, 2, 4, 5, and 7 Using HCOOH, HCOONa, or CH₃CH(CH₃)OH as Reducing Agent^f

Entry	Catalyst	%Con.	TOF (h ⁻¹)	% Selectivity		
						
1	CpRu(PTA)(PPh ₃)Cl	47.9	0.7	100	0.0	0.0
2 ^a	CpRu(PTA)(PPh ₃)Cl	39.8	0.6	65.1	0.0	34.9
3 ^b	CpRu(PTA) ₂ Cl	81.3	2.7	100	0.0	0.0
4 ^{a,b}	CpRu(PTA) ₂ Cl	14.0	0.5	73.5	0.0	26.5
5	DpRu(PTA) ₂ Cl	93.6	1.4	100	0.0	0.0
6 ^a	DpRu(PTA) ₂ Cl	89.5	1.4	100	0.0	0.0
7 ^c	DpRu(PTA) ₂ Cl	38.1	0.6	88.8	0.0	11.2
8 ^d	DpRu(PTA) ₂ Cl	41.5	0.6	100	0.0	0.0
9 ^c	IndRu(PTA)(PPh ₃)Cl	43.5	0.36	100	0.0	0.0
10 ^b	CpRu(PTA)(PPh ₃)H	32.4	1.2	91.7	8.3	0.0

^a 61.2 mg of HCO₂Na (0.9 mmol) used in place of HCO₂H. ^b 6 h. ^c HCO₂Na 61.2 mg (0.9 mmol); 5.3 mg of PTA added. ^d 38.2 mg of Na₂CO₃, 4 mL of H₂O, 3 mL of isopropanol in place of HCO₂H. ^e 150 μ L of 88% HCOOH, 2 mL of H₂O, 1 mL of MeOH, 24 h. ^f General conditions: 5 mol % of catalyst, 7.6 mg of chalcone, 40 μ L of 88% HCO₂H, 2 mL of H₂O, 3 mL of MeOH, 80 $^{\circ}$ C, 13 h.

(cinnamaldehyde, benzylidene acetone, and chalcone) has been accomplished using compounds 1–5 and 7 under acidic and basic conditions with various hydrogen donors. The results are contained in Tables 6–8. The hydrogenation products of these substrates are presented in Scheme 6. Cinnamaldehyde and benzylidene acetone were hydrogenated in aqueous solution, while chalcone was reduced utilizing a mixture of water and methanol for solubility reasons.

Transfer Hydrogenation of Cinnamaldehyde. Cinnamaldehyde was reduced under aqueous conditions utilizing Cp'Ru-(PTA)(PR₃)Cl (Cp' = Cp, Dp, Ind; PR₃ = PTA or PPh₃) compounds with formic acid or sodium formate as the reducing

Scheme 6. Hydrogenation Pathway for the Unsaturated Substrates (R = H, Me, Ph)

agent (Table 6). Entries 1, 2, 7, and 10 in Table 6 describe results of the transfer hydrogenation of cinnamaldehyde with the mixed

phosphine complexes $\text{Cp}^*\text{Ru}(\text{PTA})(\text{PPh}_3)\text{Cl}$ ($\text{Cp}^* = \text{Cp}, \text{Dp}, \text{Ind}$) using HCOOH as hydrogen donor. The complexes selectively reduce the $\text{C}=\text{O}$ bond prior to reduction of the $\text{C}=\text{C}$ bond. However, increasing the $[\text{HCOOH}]$ afforded hydrocinnamyl alcohol as the only detectable product (>99% selectivity, entry 2). Replacing $\text{CpRu}(\text{PTA})(\text{PPh}_3)\text{Cl}$ with $\text{CpRu}(\text{PTA})(\text{PPh}_3)\text{H}$ had little effect on catalysis, indicating it is a competent reaction intermediate, entry 3. A decrease in catalyst loading led to decreased formation of hydrocinnamyl alcohol but no change in the total conversion (see Supporting Information). A significant dependence of hydrocinnamaldehyde selectivity on catalyst concentration has been reported for $[\text{Ir}(\text{COD})\text{Cl}]_2$ stabilized by hydro(pyrazolyl)borate ligands.³⁴ Compared to $\text{CpRu}(\text{PTA})(\text{PPh}_3)\text{Cl}$ and $\text{DpRu}(\text{PTA})(\text{PPh}_3)\text{Cl}$, $\text{IndRu}(\text{PTA})(\text{PPh}_3)\text{Cl}$ is less active for the reduction of cinnamaldehyde; Table 6, entries 1, 7, and 10. $\text{CpRu}(\text{PTA})_2\text{Cl}$ in the presence of formic acid reduced cinnamaldehyde all the way down to hydrocinnamyl alcohol with high conversion (89.5%), Table 6, entry 4. Under basic conditions (HCOONa used in lieu of HCOOH) a different product distribution was obtained: 48.1% hydrocinnamaldehyde and 51.9% hydrocinnamyl alcohol at slightly lower total conversion (69.6%), Table 6, entry 5. Under different catalytic conditions, specifically a higher sodium formate concentration, Peruzzini et al. reported 85.6% selective olefin reduction with $\text{CpRu}(\text{PTA})_2\text{Cl}$ at low conversion (11.1%), as shown in entry 6.¹⁵ $\text{DpRu}(\text{PTA})_2\text{Cl}$ selectively reduces cinnamaldehyde to cinnamyl alcohol in >99% conversion with formic acid as hydrogen source (entry 8); replacing HCOOH with HCOONa results in exclusive formation of the double hydrogenation product, dihydrocinnamyl alcohol (entry 9). In the absence of catalyst, no formation of hydrogenation products was detected by GC-MS or ^1H NMR spectroscopy (entry 11).

The difference in product distribution observed between $\text{CpRu}(\text{PTA})_2\text{Cl}$ and $\text{DpRu}(\text{PTA})_2\text{Cl}$ (Table 6, entry 4 and 8) can be attributed to the influence of the different ancillary ligand; that is, Dp is a more sterically hindered and electron-donating ligand than Cp. Karam et al. recently observed a remarkable effect of steric and electronic properties of ancillary ligands on selective hydrogenation of cinnamaldehyde.³⁴ They reported a change in the selectivity toward the unsaturated alcohol using the more sterically demanding and electron-donating ligand Tp^* in lieu of Tp.

Transfer Hydrogenation of Benzylidene Acetone. The results of hydrogenation of benzylidene acetone by $\text{Cp}^*\text{Ru}(\text{PTA})(\text{PR}_3)\text{Cl}$ ($\text{Cp}^* = \text{Cp}, \text{Dp}, \text{Ind}$; $\text{PR}_3 = \text{PTA}$ or PPh_3) with HCOOH or HCOONa as the hydrogen donor are presented in Table 7. In the presence of formic acid, $\text{CpRu}(\text{PTA})(\text{PPh}_3)\text{Cl}$ catalyzed the transfer hydrogenation of benzylidene acetone, affording 55.9% 4-phenylbutan-2-one and 34.7% 1,3-diphenylpropan-1-ol (entry 1). Under the same conditions, $\text{DpRu}(\text{PTA})(\text{PPh}_3)\text{Cl}$ (entry 5) and $\text{IndRu}(\text{PTA})(\text{PPh}_3)\text{Cl}$ (entry 8) selectively reduced the $\text{C}=\text{C}$ bond of benzylidene acetone, with $\text{IndRu}(\text{PTA})(\text{PPh}_3)\text{Cl}$ demonstrating lower activity. In the presence of either formic acid (entry 2) or sodium formate (entry 3), $\text{CpRu}(\text{PTA})_2\text{Cl}$ selectively reduces the $\text{C}=\text{C}$ bond of benzylidene acetone, affording 4-phenylbutan-2-one. Similar regioselectivity has been reported for the reduction of benzylidene acetone using $\text{Cp}^*\text{Ru}(\text{PTA})_2\text{Cl}$ as the catalyst and sodium formate as the reducing agent.¹⁵ Hydrogenation of benzylidene acetone with $\text{DpRu}(\text{PTA})_2\text{Cl}$ as the catalyst resulted in 58.7% $\text{C}=\text{C}$ reduction and 41.3% $\text{C}=\text{O}$ hydrogenation in 81.4% total yield (entry 6) with HCOOH as the hydrogen donor. Upon

replacement of HCOOH for HCOONa , only the olefin reduction product was obtained in 83.7% yield (entry 7).

Transfer Hydrogenation of 1,3-Diphenylpropenone. The reduction of chalcone (1,3-diphenylpropenone) using $\text{Cp}^*\text{Ru}(\text{PTA})_2\text{Cl}$ ($\text{Cp}^* = \text{Cp}$ or Dp), $\text{Cp}^*\text{Ru}(\text{PTA})(\text{PPh}_3)\text{Cl}$ ($\text{Cp}^* = \text{Cp}$ or Ind), or $\text{CpRu}(\text{PTA})(\text{PPh}_3)\text{H}$ is presented in Table 8. Formic acid, sodium formate, or Na_2CO_3 /isopropanol were employed as reducing agents. All the complexes selectively hydrogenate the $\text{C}=\text{C}$ bond (>65% selectivity) irrespective of the reducing agent with the percent conversion ranging from 14 to 93%. The total conversion and selectivity for $\text{C}=\text{C}$ bond reduction were highest in acidic solution (HCOOH , entries 1, 3, 5, 9, 10). In basic media, hydrogenation continues onto the double hydrogenation product, 1,3-diphenylpropan-1-ol, thus lowering the selectivity for the $\text{C}=\text{C}$ bond reduction product, 1,3-diphenylpropan-1-one (entries 2, 4, 6, 8). The presence of free PTA dramatically lowers the % conversion for the hydrogenation of chalcone, suggesting that dissociation of PTA from $\text{DpRu}(\text{PTA})_2\text{Cl}$ may be involved in the mechanism (entry 7).

Hydride complexes have often been implicated as the active catalyst in hydrogenation reactions. Indeed, we have shown previously, with $\text{CpRu}(\text{PTA})_2\text{Cl}$, that under the catalytic conditions described the generation of $\text{CpRu}(\text{PTA})_2\text{H}$ is possible.¹⁴ As a consequence, $\text{CpRu}(\text{PTA})(\text{PPh}_3)\text{H}$ was tested as a catalyst for the reduction of chalcone, resulting in selective $\text{C}=\text{C}$ hydrogenation with small amounts of 1,3-diphenylprop-2-enol (8.3%) detected, entry 10. The use of $\text{CpRu}(\text{PTA})(\text{PPh}_3)\text{H}$ as the catalyst resulted in improved selectivity and higher activity relative to $\text{CpRu}(\text{PTA})(\text{PPh}_3)\text{Cl}$ (Table 8 entry 2), indicating that the hydride may, in fact, be the active catalyst.

Conclusions

We have presented here the synthesis, characterization, and reactivity of a series of ruthenium(II) PTA complexes bearing the cyclopentadienyl (Cp), 1,2-dihydropentalenyl (Dp), and indenyl (Ind) ancillary ligands. $\text{DpRu}(\text{PTA})_2\text{Cl}$ and $\text{CpRu}(\text{PTA})_2\text{Cl}$ are water-soluble and exhibit significant $\text{Ru}-\text{Cl}$ bond hydrolysis in aqueous solution, while the mixed phosphine complexes, $\text{Cp}^*\text{Ru}(\text{PTA})(\text{PPh}_3)\text{Cl}$, are somewhat soluble in acidic solution due to protonation of a PTA nitrogen, forming $[\text{Cp}^*\text{Ru}(\text{PTAH})(\text{PPh}_3)\text{Cl}]^+$. The $\text{Cp}^*\text{Ru}(\text{PTA})(\text{PPh}_3)\text{H}$ complexes have been prepared and undergo an H/D exchange reaction with CD_3OD with $t_{1/2} < 10$ min when $\text{Cp}^* = \text{Cp}$ and $t_{1/2} \approx 5.5$ days when $\text{Cp}^* = \text{Ind}$.

Compounds **1–5** and **7** were tested as catalysts for the selective transfer hydrogenation of unsaturated substrates in aqueous media. The mixed phosphine complexes, $\text{Cp}^*\text{Ru}(\text{PTA})(\text{PPh}_3)\text{Cl}$, selectively reduced the $\text{C}=\text{O}$ bond of cinnamaldehyde, and the $\text{C}=\text{C}$ bonds of benzylidene acetone and chalcone in the presence of formic acid ($\text{pH} \leq 3$). The indenyl complex **5** was less active than either the Cp (**1**) or Dp (**3**) analogues. Under acidic conditions (HCO_2H) $\text{DpRu}(\text{PTA})_2\text{Cl}$ was selective toward hydrogenation of the $\text{C}=\text{C}$ bond in chalcone and the $\text{C}=\text{O}$ bond in cinnamaldehyde and was not selective with benzylidene acetone as the substrate. In the presence of HCOONa , $\text{DpRu}(\text{PTA})_2\text{Cl}$ selectively reduced the $\text{C}=\text{C}$ bond of benzylidene acetone. In the presence of either formic acid or sodium formate $\text{CpRu}(\text{PTA})_2\text{Cl}$ afforded the saturated carbonyl or saturated alcohol, consistent with results previously reported.¹⁵ The results of this study indicate that the regioselectivity of reduction of unsaturated substrate depends on the ancillary ligand of the catalyst, the substrate, and the pH of the solution.

Acknowledgment. The authors would like to thank the Donors of the American Chemical Society Petroleum Research

(34) López-Linares, F.; Agrifoglio, G.; Labrador, Á.; Karam, A. *J. Mol. Catal.* **2004**, *207*, 115–120.

Fund for providing partial support of this project. Financial support from the National Science Foundation (CHE-0226402) is acknowledged for funding the X-ray diffractometer.

Supporting Information Available: ^{31}P and ^1H NMR spectra of all compounds as well as IR spectra for **7** and **8**; crystallographic

details of **1** and full bond lengths and angles for compounds **1** and **3–8**; and crystallographic data in cif format are available free of charge via the Internet at <http://pubs.acs.org>.

OM060892X